

Localized Molecular Orbital Studies of Chemical Reaction. II. Abstraction and Addition Reactions of Triplet Methylene

Shigeru NAGASE and Takayuki FUENO

Department of Chemistry, Faculty of Engineering Science, Osaka University, Toyonaka, Osaka 560

(Received May 13, 1976)

Energy-localized molecular orbitals (LMO) generated from UHF-INDO wave functions have been used for the studies of the mechanistic details of the abstraction and addition reactions of triplet methylene. The UHF LMO mapping procedure which we have previously developed permits a clear understanding of the nature of the chemical bonds to be formed or broken on reaction. Significance of the three-stage mechanism, which should involve the successive β - and α -spin electron delocalizations between reactants and the concomitant spin polarization of the reacting bond, is emphasized. The whole aspects of the reactions are well in accord with the customarily accepted mechanistic schemes.

In the preceding paper of this series,¹⁾ we dealt with mechanistic details of radical reactions in terms of the localized molecular orbitals (LMO). The results were found to be chemically meaningful in many respects. The success has encouraged us to take up the abstraction and addition reactions of triplet methylene, $\text{CH}_2(^3\text{B}_1)$. Specifically, we wish to elucidate the nature of the deformation of bonds due to the intermolecular interactions. To this end, we have carried out the LMO mapping analysis of the unrestricted Hartree-Fock (UHF) wave functions for the entire reacting systems on one hand and the schematic description of the movement of the LMO charge centroids with reaction on the other. Further, the UHF wave functions of the interacting systems were expanded as a superposition of various electronic configurations of reactant molecules, and their relative importances to the reaction were assessed. The results are found to be useful for the understanding of mechanistic features of the reactions in question.

Calculation Method

The canonical molecular orbitals (CMO) for isolated molecules as well as the reacting systems were calculated by the UHF method²⁾ in the INDO approximation.³⁾ The UHF LMO's were generated by the successive two-by-two rotation method⁴⁾ for α - and β -spin electrons separately. All possible two-orbital transformations were repeated until further increase in the sum of intraorbital Coulomb energies did not exceed 10^{-6} eV. Virtual CMO's were also localized by the same method.

The UHF LMO's ϕ^r for the entire reacting systems obtained at various reaction path points are mapped over the LMO's ϕ for the isolated reactant molecules:

$$\phi^r = \phi^r T^r \quad (1)$$

where T^r is a unitary matrix pertinent to the mapping, the superscript r denoting the α - or β -spin. The LMO mapping matrix T^r was obtained by the same procedure as described in a previous paper.¹⁾

The UHF ground-state wave functions at given path points can be expanded into various electronic configurations:

$$\begin{aligned} \Psi_{\text{UHF}} &= |\phi_1^\alpha \phi_1^\beta \cdots \phi_p^\alpha \phi_p^\beta \phi_{p+1}^\alpha| \\ &= C_0 \Phi_0 + \sum_K \sum_i C_{Ki} \Phi_{Ki} \end{aligned} \quad (2)$$

where Φ_0 is the ground configuration and where Φ_{Ki} is the i -th configuration of type K —local excitation (LE) of reactant molecule, charge transfer (CT) from reactant to $^3\text{CH}_2$, back charge transfer (BCT) from $^3\text{CH}_2$ to reactant, and so on.¹⁾ The configurational coefficients, C_0 and C_{Ki} 's, were calculated by the technique similar to the one used by Baba *et al.*⁵⁾ All computations were carried out on a FACOM 230-60 at the Kyoto University Computation Center.

Results and Discussion

A. Characteristics of the UHF-LMO's of Methylene.

It is recognized that methylene (CH_2) can exist in both singlet ($^1\text{A}_1$) and triplet ($^3\text{B}_1$) states. The bond angles calculated by the INDO method for a fixed bond length ($R_{\text{CH}} = 1.094$ Å) are 107 and 132°, respectively,³⁾ which are both in good agreement with observations (102.4 and 136°, respectively^{6–8)}). The LMO's which we obtained at these calculated equilibrium angles are shown in Table 1, where $\text{CH}_2(^3\text{B}_1)$ is assumed to have two more α -spin electrons than β -spin ones. It can be seen that each LMO is certainly little delocalized (less than 1%).

The total energy E of methylene can be expressed as the sum of contributions from individual occupied LMO's, provided the nuclear charge of each atom is assumed to be expressible in the form^{9–11)}

$$Z_A = \sum_i Z_{i,A} \quad (3)$$

where $Z_{i,A}$ is the part of the nuclear charge on atom A partitioned to the i -th LMO. The value of $Z_{i,A}$ is taken to be equal to 1 for an unpaired LMO as well as an LMO localized mainly around two atoms, whereas $Z_{i,A} = 2$ for a lone-pair LMO. The component energies ϵ_i^r thus derived are given by

$$\epsilon_i^r = \frac{1}{2} \langle \phi_i^r | \mathbf{F}^r + \mathbf{H}^c | \phi_i^r \rangle + c_i \sum_A \sum_B \sum_j e^2 Z_{i,A} Z_{j,B} / R_{AB} \quad (4)$$

where \mathbf{F}^r and \mathbf{H}^c are the Hartree-Fock and core Hamiltonian operators, respectively; R_{AB} is the inter-nuclear distance between atoms A and B ; and c_i is a constant which is 1/2 for the i -th α -spin counterpart of a β -spin LMO and 1 for an unpaired radical-center LMO.

Figures 1 and 2 show the variations in ϵ_i^r of various filled LMO's of the singlet and triplet methylenes, respectively, with the bond angle $\angle\text{HCH}$. The numbers

TABLE 1. LOCALIZED ORBITALS FOR THE SINGLET AND TRIPLET METHYLENES

LMO ^{a)}		AO coefficients					
		Cs	Cp _x	Cp _y	Cp _z	H _a	H _b
		CH ₂ (¹ A ₁)					
Occupied	CH _a	0.399	0.353	0.475	0.000	0.700	-0.011
	L	0.715	-0.693	0.000	0.000	-0.060	-0.060
Vacant	CH _a *	0.307	0.380	0.506	0.000	-0.710	-0.012
	L*	0.000	0.000	0.000	1.000	0.000	0.000
		CH ₂ (³ B ₁)					
Occupied	CH _a ^α	0.348	0.404	0.497	0.000	0.684	-0.027
	CH _a ^β	0.518	0.129	0.471	0.000	0.701	-0.045
	N _±	0.517	-0.482	0.000	±0.707	0.023	0.023
Vacant	CH _a ^{α*}	0.335	0.324	0.503	0.000	-0.728	-0.025
	CH _a ^{β*}	0.411	0.236	0.527	0.000	-0.704	-0.038
	N _± *	0.250	-0.654	0.000	±0.707	-0.069	-0.069

a) See Figs. 1 and 2.

appended indicate the values of α for hybridization (sp^{α}) of the carbon orbitals involved.

Comparison of Fig. 1 with Fig. 2 shows that the energies ϵ_i' have a roughly similar pattern of angular variations for both spin states. The lone-pair (L) and unpaired (N) orbital energies have the greatest angular variations and are decreased as the bond angle decreases. On the contrary, the C-H bond energies for both spin states increase with the decreasing bond angle. In other words, the nonbonding orbitals tend to make the methylene molecule bent, while the C-H bond orbitals are energetically in favor of the linear geometry. The equilibrium bond angles would be a compromise between these two opposing contributions. The results are in accord with those obtained by the electrostatic force theory,¹²⁾ in which the former contribution is ascribed to the "atomic dipole" force and the latter, to the "exchange" force.

Here, considerations of the spatial arrangement of the

C-H bond orbitals themselves seem to be in order. In the triplet methylene, the LMO's for the α -spin electrons can be described roughly as tetrahedral (sp^3) in type while those for the β -spin electrons as linear (sp). Pauling¹³⁾ pointed out qualitatively that the two (C-H) ^{α} bond orbitals would tend to bring the HCH bond angle to 90° while the two (C-H) ^{β} bond orbitals, to 180°. The directions of the C-H bond orbitals obtained by the present treatment for varying bond angle are as illustrated in Fig. 3. Deviations of the direction of bond orbitals from that of the C-H bonds may be taken as reflecting the force with which the orbitals attract the H nucleus. It would then appear as though the bond angle were determined by the balance between the attractive forces from the (C-H) ^{α} and (C-H) ^{β} bond orbitals. Thus, at the equilibrium bond angle, the hydrogen atom is situated nearly on the bisector of the angle between the bond orbitals. For the singlet state, things are much simpler; only when the equilibrium

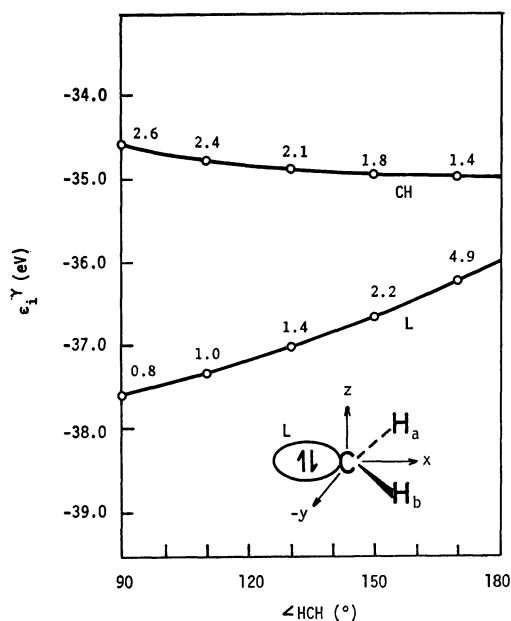


Fig. 1. Variations of the bond energy and hybridization with the bond angle (\angle HCH) for the singlet methylene.

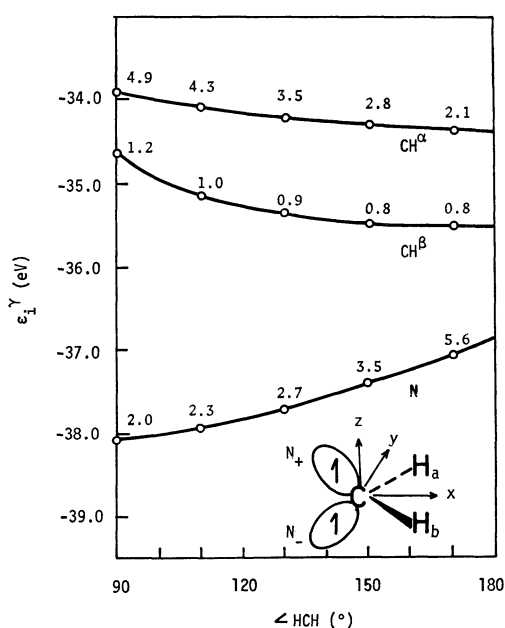


Fig. 2. Variations of the bond energy and hybridization with the bond angle (\angle HCH) for the triplet methylene.

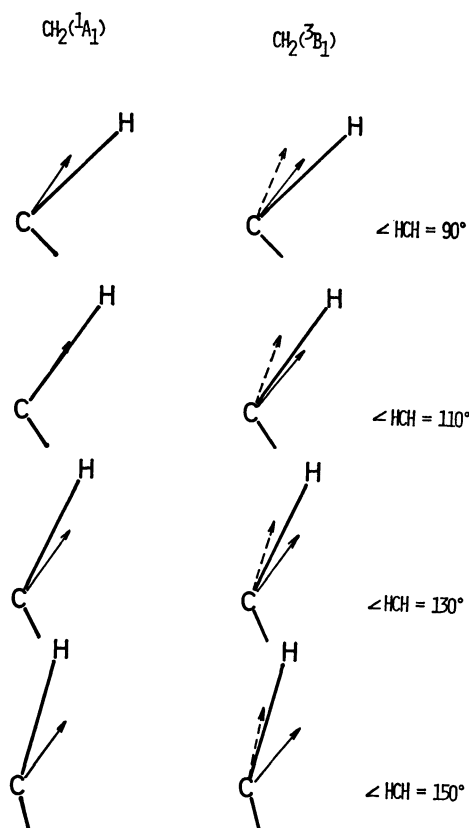


Fig. 3. Directions of the C-H bond orbitals for $1,3\text{-CH}_2$. The solid and broken arrows for 3CH_2 show the directions of the α - and β -spin C-H bond orbitals, respectively.

bond angle is reached, can the hydrogen atom locate itself in the direction of the (C-H) bond orbital. These results may serve as a useful guide for the prediction of the changes in nuclear motions during chemical reactions.

B. Abstraction Reaction. We wish to examine the reaction of triplet methylene with methane as a prototype of abstraction reactions. The reaction is considered to proceed *via* a linear transition state¹⁴⁾ as shown in Fig. 4. This was indeed confirmed by the calculations¹⁵⁾ of the intermolecular interaction energy based on our intermolecular perturbation method.¹⁶⁾ A similar transition state geometry has been assumed for the hydrogen abstraction reaction of triplet methylene from molecular hydrogen.¹⁷⁾

The main purpose of this study is to analyze the alteration in electronic structure of molecules during

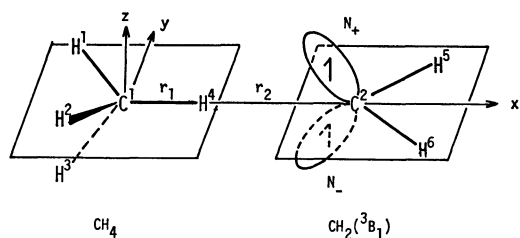


Fig. 4. Coordinate system for the abstraction reaction of methane by triplet methylene.

reaction rather than the change in the total energy, and to interpret it in an orderly manner in terms of the LMO mappings. We specify the reaction path with the notation (r_1, r_2) , where r_1 is the distance in units of Å between carbon C^1 and hydrogen H^4 , while r_2 is that between carbon C^2 and hydrogen H^4 (Fig. 4). Calculations were carried out at model path points A(1.09, 2.5), B(1.09, 2.0), C(1.09, 1.5), and D(1.29, 1.3),¹⁸⁾ where 1.09 Å is the equilibrium C-H distance of methane.¹⁹⁾

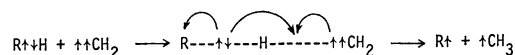
Variations in hybridization during the reaction are shown in Table 2. It is seen that the bond orbitals $\text{C}^1\text{-H}^1$ and $\text{C}^1\text{-H}^4$ of methane suffer variations in hybridization in different manners. The α -spin $\text{C}^1\text{-H}^4$ bond destined to be cleaved diminishes in p character as the reaction proceeds. In the meantime, the remaining three α -spin C-H bonds gain p character to make up the decrease in p character of the α -spin $\text{C}^1\text{-H}^4$ bond. On the other hand, the β -spin $\text{C}^1\text{-H}^4$ bond gains p character, being accompanied by the decrease in p character of the remaining three β -spin C-H bonds. As for the methylene molecule, the p character of both the α - and β -spin C-H bonds tends to be increased while that for the unpaired α -spin orbitals is decreased. It is only the $\text{C}^1\text{-H}^4$ bond that suffers drastic change in form during the reaction.

TABLE 2. VARIATIONS IN HYBRIDIZATION^{a)} OF THE CARBON ATOMS IN THE $\text{CH}_4\text{-}^3\text{CH}_2$ SYSTEM^{b)}

Path point	CH_4				$^3\text{CH}_2$		
	$\text{C}^1\text{-H}^1$		$\text{C}^1\text{-H}^4$		$\text{C}^2\text{-H}^5$		N_+
	α -spin	β -spin	α -spin	β -spin	α -spin	β -spin	α -spin
$\infty^c)$	2.68	2.68	2.68	2.68	3.45	0.89	2.73
(A)	2.68	2.66	2.66	2.69	3.45	0.89	2.73
(B)	2.72	2.62	2.59	2.76	3.46	0.91	2.69
(C)	2.87	2.47	2.31	3.10	3.66	0.99	2.53

a) The entries are the values of x for the hybridization sp^x . b) See Fig. 4. c) Isolated reactants.

Shown in Fig. 5 are the movements of the centroids of the LMO charge distributions with the progress of reaction. The approach of two unpaired electrons of the methylene carbon decouples the electron pairing in the $\text{C}^1\text{-H}^4$ bond. The β -spin electron moves toward the H^4 atom while the α -spin electron, in the opposite direction. This separation of the α - and β -spin electrons will effectively weaken (and eventually break) the bond. Meanwhile, the β -spin electron begins to be coupled with one of the α -spin electrons of CH_2 . The situation is closely related to the conventional representation as follows:



A better insight into the mechanism of bond rearrangement can be obtained from the results of LMO mapping analysis (Table 3). The bonds other than the $\text{C}^1\text{-H}^4$ bond of methane and the N_\pm orbitals of methylene suffer little deformation during the reaction. The α -spin electrons in N_\pm orbitals are delocalized mainly into the antibonding orbital $(\text{C}^1\text{-H}^4)^*$, which will weaken the $\text{C}^1\text{-H}^4$ bond. On the other hand, the β -spin orbital

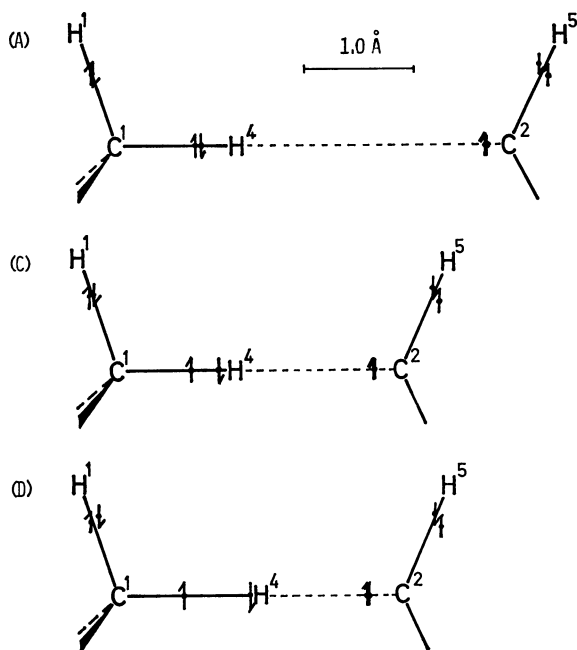


Fig. 5. Top view of the centroids of localized molecular orbitals in the $\text{CH}_4\text{-CH}_2(^3\text{B}_1)$ system at the path points (A), (C), and (D).

($\text{C}^1\text{-H}^4$) mixes first with the vacant unpaired orbital N^* of methylene in a strongly bonding way and then with the antibonding orbital ($\text{C}^1\text{-H}^4$)* with a negative sign. The corresponding α -spin orbital allows the orbital ($\text{C}^1\text{-H}^4$)* to mix into it with a positive sign. The mixing of the antibonding orbital ($\text{C}^1\text{-H}^4$)* into the corresponding α - and β -spin bonding orbitals ($\text{C}^1\text{-H}^4$) in different signs is what is usually called "spin polarization." The spin polarization induces an excess

TABLE 3. LMO MAPPING ANALYSIS OF THE HYDROGEN ABSTRACTION OF $^3\text{CH}_2$ FROM CH_4

Spin	Path point	Mapped LMO ^{a)}
$\text{C}^1\text{-H}^4$		
α	(A)	$0.999(\text{C}^1\text{H}^4) + 0.005(\text{C}^1\text{H}^4)^*$
	(B)	$0.999(\text{C}^1\text{H}^4) + 0.023(\text{C}^1\text{H}^4)^* - 0.002[(\text{N}_+) + (\text{N}_-)]$
	(C)	$0.989(\text{C}^1\text{H}^4) + 0.088(\text{C}^1\text{H}^4)^* - 0.008[(\text{N}_+) + (\text{N}_-)]$
	(D)	$0.946(\text{C}^1\text{H}^4) + 0.301(\text{C}^1\text{H}^4)^* - 0.051[(\text{N}_+) + (\text{N}_-)]$
β	(A)	$0.998(\text{C}^1\text{H}^4) - 0.003(\text{C}^1\text{H}^4)^*$
	(B)	$0.986(\text{C}^1\text{H}^4) - 0.017(\text{C}^1\text{H}^4)^* + 0.049[(\text{N}_+)^* + (\text{N}_-)^*]$
	(C)	$0.937(\text{C}^1\text{H}^4) - 0.056(\text{C}^1\text{H}^4)^* + 0.115[(\text{N}_+)^* + (\text{N}_-)^*]$
	(D)	$0.866(\text{C}^1\text{H}^4) - 0.177(\text{C}^1\text{H}^4)^* + 0.237[(\text{N}_+)^* + (\text{N}_-)^*]$
N_\pm		
α	(A)	$0.999(\text{N}_\pm) - 0.024(\text{C}^1\text{H}^4)^*$
	(B)	$0.998(\text{N}_\pm) - 0.052(\text{C}^1\text{H}^4)^* + 0.003(\text{C}^1\text{H}^4)$
	(C)	$0.992(\text{N}_\pm) - 0.116(\text{C}^1\text{H}^4)^* + 0.025(\text{C}^1\text{H}^4)$
	(D)	$0.962(\text{N}_\pm) - 0.236(\text{C}^1\text{H}^4)^* + 0.128(\text{C}^1\text{H}^4)$

a) For the LCAO expressions of the $\text{C}^1\text{-H}^4$ bond LMO's, (C^1H^4) and (C^1H^4)* of isolated methane, see Table 1 of Ref. 1

α -spin density around the carbon C^1 and an excess β -spin density around the hydrogen H^4 .

All the above arguments converge into a concept of three-stage mechanism as follows: The main bond deformation caused at the initial stage of reaction is due to the mixing of the β -spin $\text{C}^1\text{-H}^4$ orbital into the vacant unpaired orbital N_\pm^* . At the middle stage, the mixing of the α -spin N_\pm orbital into the antibonding orbital ($\text{C}^1\text{-H}^4$)* develops, to form a three-center bond. As the reaction approaches the final stage, the mixing of the α -spin orbital ($\text{C}^1\text{-H}^4$) into the antibonding orbital ($\text{C}^1\text{-H}^4$)* becomes dominant. Thus, in the first place, a β -spin electron is transferred from methane to methylene; next, back transfer of an α -spin electron from methylene to methane takes place; and finally, local excitation in the bond to be broken becomes appreciable. The first stage can be termed the electrophilic stage of the reaction. From the viewpoint of spin properties, the first and second stages may be envisaged as the "spin delocalization" stage, which operates to drive the two reactant molecules close to each other, thus forming a three-center bond over C^1 , H^4 , and C^2 . Cleavage of the old bond is effected primarily by the last stage, *i.e.*, the "spin polarization" stage. The spin polarization is in effect equivalent to the "triplet excitation" noted in the intermolecular configuration interaction treatments.^{1,20}

In connection with the above statement, we briefly consider the reaction of the triplet methylene with CH_3X ($\text{X}=\text{F}$ or Cl). Triplet methylene attacks substrates containing both hydrogen and halogen atoms in a selective manner; it abstracts a hydrogen atom rather than a halogen atom.²¹ The calculated triplet excitation energies²² from the bonding (C-H) to antibonding (C-H)* orbital are 17.1 and 17.3 eV for CH_3F and CH_3Cl , respectively. Those from (C-F) and (C-Cl) to (C-F)* and (C-Cl)* are 24.0 and 19.1 eV, respectively. Thus, we may anticipate the spin polarization effect to be larger in the C-H bond rather in the C-F or C-Cl bond. Spin density distributions in

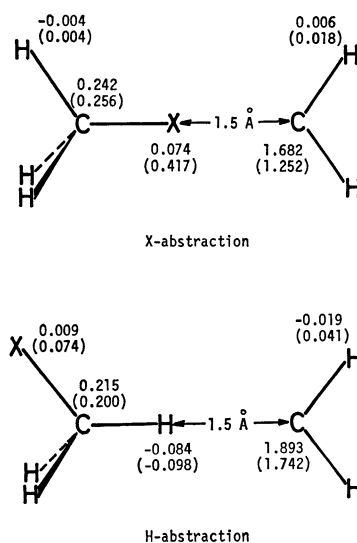


Fig. 6. Spin density distributions in the $\text{CH}_3\text{X-CH}_2(^3\text{B}_1)$ system ($\text{X}=\text{F}$ or Cl). The entries given in parentheses are the values for the case of $\text{X}=\text{Cl}$.

the reaction systems lend support to this view (Fig. 6).

Apparently, the distributions are $\dot{\text{C}}\cdots\dot{\text{X}}\cdots\dot{\text{C}}$ in the case of the halogen abstraction and $\dot{\text{C}}\cdots\dot{\text{H}}\cdots\dot{\text{C}}$ for the hydrogen abstraction. Thus, the triplet excitation energy in the bond as well as the spin density distribution may be a useful guide for predicting the relative ease of the bond cleavage.

C. Addition Reaction. The reaction here studied is the addition of triplet methylene to the double bond of ethylene. Characteristics of this particular reaction was already investigated by Hoffmann²³⁾ in terms of the extended Hückel molecular orbitals. The reaction path was more thoroughly examined by Bodor *et al.*¹⁴⁾ using the MINDO/2 method. We here choose to employ the path similar to that of Bodor *et al.* for our purpose.

The relative positions of methylene and ethylene during the reaction are specified as shown in Fig. 7. The middle of the ethylene double bond was taken as the origin of the coordinate. The carbons C¹ and C² of ethylene are put on the x axis, and the carbons C¹, C² and C³ are placed on the xz plane. The entire system is assumed to be symmetric with respect to this plane. The geometry of the system is characterized by the notation (r, θ, ψ, ω) in units of Å and degree. The path points considered are A(3.5, 90, 90, 0), B(2.4, 85, 90, 0), C(2.0, 80, 80, 0), D(1.9, 65, 75, 0), E(1.9, 50, 60, 0), and F(1.9, 50, 60, 30).

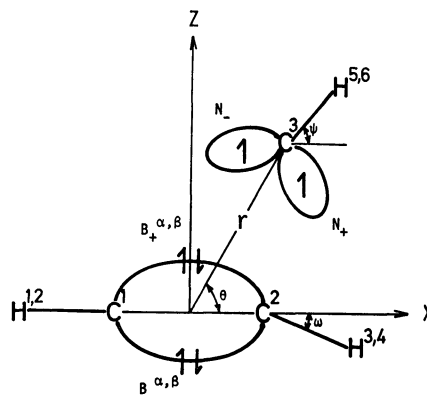


Fig. 7. Coordinate system (side view) for describing the relative position of $\text{CH}_2(^3B_1)$ and $\text{CH}_2=\text{CH}_2$.

The LMO calculations for the ethylene molecule provide two equivalent banana bonds for the description of the double bond; one (B_+) lies above the molecular plane while the other (B_-) below it. The banana bonds associated with the α - and β -spin electrons are specified as B_{\pm}^{α} and B_{\pm}^{β} , respectively. The triplet methylene has two unpaired orbitals N_+ and N_- as has been mentioned earlier.

When reaction takes place, these particular LMO's suffer the greatest deformation. Table 4 gives the results of the LMO mapping analysis at path points (B)

TABLE 4. LMO MAPPING ANALYSIS OF THE ADDITION OF $^3\text{CH}_2$ TOWARD C_2H_4

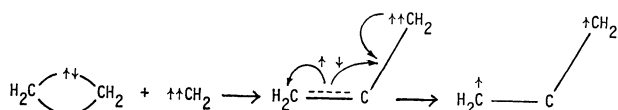
Spin	Path point	Mapped LMO ^{a)}
B_-		
α	(B)	1.000(B_-)
	(C)	0.982(B_-) + 0.170(B_+)
	(D)	0.859(B_-) + 0.508(B_+)
	(E)	0.819(B_-) + 0.570(B_+)
	(F)	0.819(B_-) + 0.570(B_+)
β	(B)	0.990(B_-) + 0.079(B_+)
	(C)	0.949(B_-) + 0.303(B_+)
	(D)	0.882(B_-) + 0.456(B_+)
	(E)	0.838(B_-) + 0.527(B_+)
	(F)	0.838(B_-) + 0.527(B_+)
B_+		
α	(B)	0.998(B_+) - 0.023(B_-) + 0.017(N_+) [*] - 0.014(N_-) [*]
	(C)	0.965(B_+) - 0.150(B_-) + 0.132(N_+) [*] - 0.116(N_-) [*]
	(D)	0.762(B_+) - 0.433(B_-) + 0.333(N_+) [*] - 0.294(N_-) [*]
	(E)	0.701(B_+) - 0.467(B_-) + 0.374(N_+) [*] - 0.344(N_-) [*]
	(F)	0.701(B_+) - 0.467(B_-) + 0.374(N_+) [*] - 0.344(N_-) [*]
β	(B)	0.963(B_+) - 0.046(B_-) - 0.014(N_+) [*] + 0.011(N_-) [*] + 0.198(N_+) [*] + 0.174(N_-) [*]
	(C)	0.857(B_+) - 0.241(B_-) - 0.069(N_+) [*] + 0.053(N_-) [*] + 0.298(N_+) [*] + 0.326(N_-) [*]
	(D)	0.736(B_+) - 0.354(B_-) - 0.136(N_+) [*] + 0.113(N_-) [*] + 0.392(N_+) [*] + 0.353(N_-) [*]
	(E)	0.679(B_+) - 0.398(B_-) - 0.157(N_+) [*] + 0.140(N_-) [*] + 0.433(N_+) [*] + 0.324(N_-) [*]
	(F)	0.679(B_+) - 0.398(B_-) - 0.157(N_+) [*] + 0.140(N_-) [*] + 0.433(N_+) [*] + 0.324(N_-) [*]
N_+		
α	(B)	0.995(N_+) + 0.001(N_-)
	(C)	0.950(N_+) + 0.004(N_-) + 0.066(B_+) - 0.040(B_-) - 0.218(N_+) [*] + 0.193(N_-) [*]
	(D)	0.828(N_+) + 0.176(N_-) + 0.246(B_+) - 0.160(B_-) - 0.302(N_+) [*] + 0.282(N_-) [*]
	(E)	0.712(N_+) + 0.321(N_-) + 0.289(B_+) - 0.213(B_-) - 0.302(N_+) [*] + 0.313(N_-) [*]
	(F)	0.712(N_+) + 0.321(N_-) + 0.289(B_+) - 0.213(B_-) - 0.302(N_+) [*] + 0.313(N_-) [*]
N_-		
β	(B)	0.999(N_-) - 0.002(N_+)
	(C)	0.996(N_-) - 0.005(N_+)
	(D)	0.947(N_-) - 0.265(N_+)
	(E)	0.869(N_-) - 0.457(N_+)
	(F)	0.869(N_-) - 0.457(N_+)

a) For the LCAO expressions of the banana bond LMO's B_{\pm} and B_{\pm}^* of isolated ethylene, see Table 4 of Ref. 1

to (E). As is naturally expected, the $B-\alpha$, $B-\beta$, $B+\alpha$, and $N-$ bonds are responsible primarily for the intramolecular bond rearrangement, while the $B+\beta$ and $N+$ orbitals, for the intermolecular bond formation. Here also, the mixing of the $B+\alpha$ and $B+\beta$ bonds with the anti-bonding $B+*$ and $N-*$ bonds takes place with opposite signs, a situation which is equivalent to an inducement of triplet excitation in the double bond.¹⁾

The addition reaction of triplet methylene also conforms to a three-stage mechanism. As can be inferred from Table 4, triplet methylene initially approaches ethylene as a β -spin acceptor. Next, it comes to behave as an α -spin donor. Finally, local excitation in the ethylene molecule becomes appreciable. The β - and α -spin electron transfers must be the major origin of the formation of the new C^2-C^3 bond. The local excitation, *i.e.*, spin polarization in the C^1-C^2 bond should be a factor most effective to the cleavage of the $B+$ bond.

The results described above can be illustrated pictorially by the schematic representation of the centroids of LMO charge distributions (Fig. 8). Again, the schematic description is in accord with the conventional scheme:



The paired electrons which existed in the $B-$ bond are slightly decoupled and migrate toward the mid-point of the carbons C^1 and C^2 to form a single bond. The

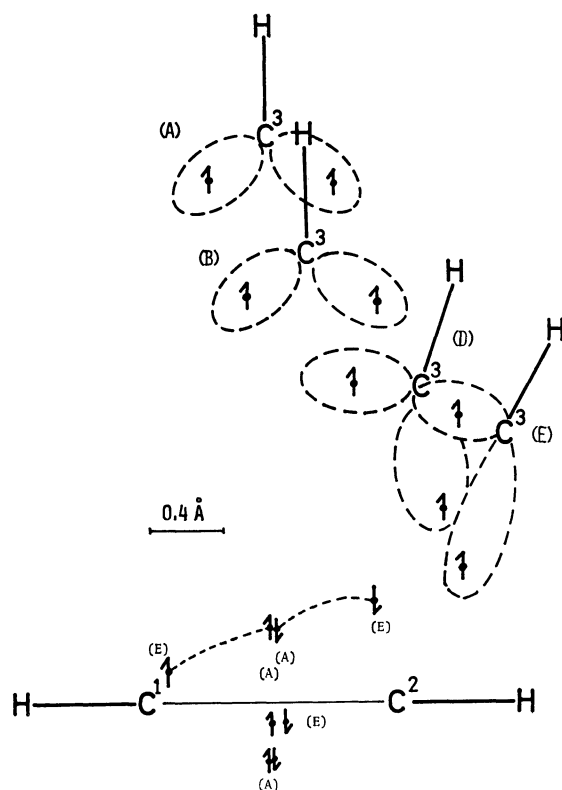


Fig. 8. Schematic representation of the centroids of LMO charge distributions at path points (A)—(E) in the addition reaction of triplet methylene to ethylene.

paired electrons which existed in the $B+$ bond are highly decoupled; the α -spin electron migrates onto the carbon C^1 to form a radical center there, while the β -spin electron migrates toward the mid-point of the carbons C^2 and C^3 to make a pair with one of the two unpaired electrons of methylene, leaving the other unpaired electron to form another radical center on C^3 .

Listed in Table 5 are the total weights $\sum_i C_{Ki}^2$ of various types of configurations K contributing to Φ_{UHF} at different reaction path points. That the reaction proceeds by the three-stage mechanism can be perceived here even more clearly. Thus, the most dominant configuration to be mixed with Φ_G at initial stages of reaction is Φ_{CT} , the β -spin delocalization from ethylene to CH_2 . This is followed up by the mixing of Φ_{BCT} , the α -spin delocalization from CH_2 to ethylene. Finally, the contribution of Φ_{LE} due to the α -spin, and hence triplet, excitation on ethylene becomes appreciable.

TABLE 5. TOTAL WEIGHTS OF THE COMPOSITE CONFIGURATIONS IN THE ADDITION OF TRIPLET METHYLENE (M) TO ETHYLENE (E)

Path point	Spin	C_G^2 (EM)	$\sum_i C_{LE,i}^2$ (E* M)	$\sum_k C_{CT,k}^2$ (E+ $M-$)	$\sum_l C_{BCT,l}^2$ (E- $M+$)	$\sum_j C_{LE,j}^2$ (EM*)
(A)	α	0.998	0.000	0.000	0.000	0.000
	β		0.000	0.002	0.000	0.000
(B)	α	0.896	0.001	0.003	0.009	0.001
	β		0.001	0.085	0.000	0.001
(C)	α	0.648	0.026	0.010	0.073	0.008
	β		0.008	0.179	0.001	0.008
(D) ^{a)}	α	0.354	0.082	0.005	0.178	0.001
	β		0.019	0.176	0.001	0.009

a) Other highly-transferred and highly-excited configurations are also mixed into the ground configuration.

If triplet methylene approached ethylene by way of the least motion with the C_{2v} symmetry ($\theta=\phi=90^\circ$), no new pairing of opposite spins would be possible between them and the bonded electron pair in $B+$ could not be decoupled with ease. This was in fact confirmed by separate calculations. The situation is much the same as in the addition of methyl radical to ethylene, which has been discussed previously.¹⁾ The steric course of reaction should thus be dependent upon how smoothly the interchange of pairing of opposite spins can take place.

References

- 1) S. Nagase, K. Takatsuka, and T. Fueno, *J. Am. Chem. Soc.*, **98**, 3838 (1976).
- 2) J. A. Pople and R. K. Nesbet, *J. Chem. Phys.*, **22**, 571 (1954).
- 3) J. A. Pople and D. L. Beveridge, "Approximate Molecular Orbital Theory," McGraw-Hill, New York (1970).
- 4) C. Edmiston and K. Ruedenberg, *Rev. Mod. Phys.*, **35**, 457 (1963); *J. Chem. Phys.*, **43**, 597 (1965).
- 5) H. Baba, S. Suzuki, and T. Takemura, *J. Chem. Phys.*, **50**, 7078 (1969).
- 6) G. Herzberg and J. W. C. Johns, *Proc. R. Soc. London, Ser. A*, **295**, 107 (1966); *J. Chem. Phys.*, **54**, 2276 (1971).
- 7) E. Wasserman, V. J. Kuck, R. S. Hutton, and W. A.

Yager, *J. Am. Chem. Soc.*, **92**, 7491 (1970).

8) R. A. Bernheim, H. W. Bernard, P. S. Wang, L. S. Wood, and P. S. Skell, *J. Chem. Phys.*, **53**, 1280 (1970).

9) J. M. Parks and R. G. Parr, *J. Chem. Phys.*, **28**, 335 (1958).

10) T. L. Allen and H. Shull, *J. Chem. Phys.*, **35**, 1644 (1961).

11) W. England and M. S. Gordon, *J. Am. Chem. Soc.*, **93**, 4649 (1971).

12) H. Nakatsuji, *J. Am. Chem. Soc.*, **95**, 345, 354, 2084 (1973).

13) L. Pauling in "Molecular Orbitals in Chemistry, Physics, and Biology," P.-O. Löwdin and B. Pullman, Ed., Academic Press, New York (1964) p. 207.

14) N. Bodor, M. J. S. Dewar, and J. S. Wasson, *J. Am. Chem. Soc.*, **94**, 9095 (1972).

15) S. Nagase and T. Fueno, *Theor. Chim. Acta*, **41**, 59 (1976).

16) T. Fueno, S. Nagase, K. Tatsumi, and K. Yamaguchi, *Theor. Chim. Acta*, **26**, 431 (1972); S. Nagase and T. Fueno,

ibid., **35**, 217 (1974).

17) C. P. Baskin, C. F. Bender, C. W. Bauschlicher, Jr., and H. F. Schaefer III, *J. Am. Chem. Soc.*, **96**, 2709 (1974).

18) The points A to D, which have been selected rather arbitrarily in this work, may not fall exactly on the reaction path to be obtained by rigorous calculations of the potential energy surface. Nevertheless, we believe that the qualitative features of the reaction which are pointed out herewith would not be affected seriously by more rigorous treatments of the reaction.

19) H. C. Allen and E. K. Plyler, *J. Chem. Phys.*, **26**, 972 (1957).

20) A. D. McLachlan, *Mol. Phys.*, **5**, 51 (1962).

21) H. D. Roth, *J. Am. Chem. Soc.*, **93**, 1527, 4935 (1971); **94**, 1400 (1972).

22) As the INDO parametrization is not available in the original method for the second row atoms, we employed the CNDO approximation including d orbitals.³⁾

23) R. Hoffmann, *J. Am. Chem. Soc.*, **90**, 1475 (1968).
